Journal of Macromolecular Science, Part A
Publication details, including instructions for authors and subscription information:
http://www.informaworld.com/smpp/title~content=t713597274

Photochemistry and Photopolymerization Activity of Diaryliodonium Salts

J. P. Fouassier[a]; D. Burr[a]; J. V. Crivello[b]
[a] Laboratoire de Photochimie, Générale Unité Associée au CNRS 431 Ecole Nationale Supérieure de Chimie, Mullhouse Cedex, France [b] School of Science-Department of Chemistry, Rensselaer Polytechnic Institute, Troy, New York, USA

To cite this Article Fouassier, J. P. , Burr, D. and Crivello, J. V.(1994) 'Photochemistry and Photopolymerization Activity of Diaryliodonium Salts', Journal of Macromolecular Science, Part A, 31: 6, 677 — 701

To link to this Article: DOI: 10.1080/10601329409349748

URL: http://dx.doi.org/10.1080/10601329409349748

J.M.S.—PURE APPL. CHEM., A31(6), pp. 677–701 (1994)

PHOTOCHEMISTRY AND PHOTOPOLYMERIZATION ACTIVITY OF DIARYLIODONIUM SALTS

J. P. FOUASSIER and D. BURR

Laboratoire de Photochimie Générale
Unité Associée au CNRS 431
Ecole Nationale Supérieure de Chimie
68093 Mullhouse, Cedex, France

J. V. CRIVELLO*

School of Science — Department of Chemistry
Rensselaer Polytechnic Institute
Troy, New York 12180-3590, USA

Key Words: Iodonium salts; Photosensitization; Thioxanthone; Photolysis; Photoinitiated cationic polymerization

ABSTRACT

An investigation of the direct and thioxanthone photosensitized photolysis of substituted diaryliodonium salts was carried out. The rate constants for the photolysis processes involved, acidity release, and rates of polymerization of cationic monomers in films have been measured and are discussed. The addition of thioxanthone derivatives as photosensitizers was found to have little effect on the polymerization efficiency.

INTRODUCTION

In the past few years there has been an increasing interest in the study of photopolymerization reactions [1–3]. The key role played by the photoinitiator, especially in free-radical polymerizations, has been the subject of much study, and the mechanisms of initiation have been elucidated [4-7]. The recent development of onium salts as cationic photoinitiators [8, 9] has generated a considerable number of investigations into the mechanism and photochemical reactivity of these photoinitiators. Articles have already appeared reporting on the mechanism of the direct photolysis of diphenyliodonium (DPI) and triphenylsulfonium (TPS) salts [10-12], analysis of the excited species formed [13, 14], and the sensitized decomposition of DPIs in the presence of such photosensitizers as benzophenone [15], acetophenone [14], benzoin alkyl ethers [16, 17], benzoyl triphenylphosphine oxide [17], anthracene [13], chlorothioxanthone [18], pyrene [8], Ru^{2+} complexes [18], and various thioxanthone derivatives [19, 20].

Although the mechanisms of both the direct and photosensitized photolysis of onium salts seem well established, there has been little mention in the literature of attempts to relate the photochemical reactivity of various photoinitiators to their efficiency in cationic photopolymerization. The present article is devoted to this topic, and the photopolymerization efficiency will be discussed in terms of the excited state reactivity of various substituted diaryliodonium salts in the presence and absence of a number of substituted thioxanthone (TX) photosensitizers.

EXPERIMENTAL

Materials

Shown in Table 1 are the structures of the diaryliodonium salts (DPIs), thioxanthone (TX) photosensitizers, and epoxide monomers used in this research. The DPIs were prepared according to procedures which were described previously [8]. The thioxanthone photosensitizers and epoxide monomers were obtained from the Ciba-Geigy Corporation.

Methods

The techniques and instrumentation used in the time-resolved laser-spectroscopy measurements were conducted as described previously [21]. Short light pulses of 3 ns at 355 nm were produced by a Nd-YAG laser. All the measurements were made on thoroughly deoxygenated solutions produced by bubbling nitrogen through the solutions at 20°C. Duplicate experiments and measurements were conducted in all cases to check for reproducibility. Transient absorption spectra were taken point-by-point with a suitable wavelength interval by varying the monochromator setting.

The spectroscopic absorption and fluorescence measurements were made using, respectively, Beckman DU-7 UV-visible and Perkin-Elmer LS-5 Luminescence spectrometers. The photolysis of the DPIs were carried out in methanol in closed quartz cells employing a 125-W HPK medium pressure mercury arc lamp equipped with different filters to obtain monochromatic light. The potential different (ΔV, mV) in the solution was monitored during the photolysis. Using these values, the acidity of the medium could be calculated. In typical photolysis experiments, the optical density of the thioxanthone derivatives was adjusted to be in the 0.4-0.5 range at λ = 366 nm, and the concentration of the DPI in the reaction medium was 10^{-2} M.

TABLE 1A. Diaryliodonium Salts Used in These Investigations

Name	Notation	Structure	
Diphenyliodonium PF_6^-, AsF_6^-	1	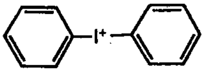	PF_6^-, AsF_6^-
3,3′-Dinitrodiphenyliodonium AsF_6^-	2	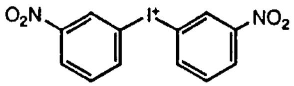	AsF_6^-
4-Methoxyphenylphenyliodonium AsF_6^-	3	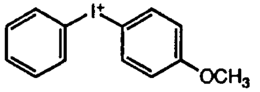	AsF_6^-
Biphenyleneiodonium AsF_6^-	4	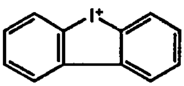	AsF_6^-
3,3′,4,4′-Tetramethyldiphenyliodonium AsF_6^-	5	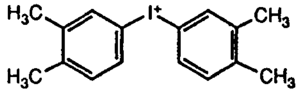	AsF_6^-
3-Fluorenylphenyliodonium AsF_6^-	6	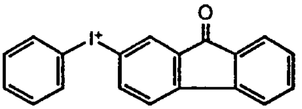	AsF_6^-

Photopolymerizations were monitored by infrared spectroscopy. An 80-W mercury arc lamp was used to irradiate the samples. The intensity at the surface of the samples was typically 100 mW/cm^2. The samples consisted of 12 μm thick liquid films containing 1 and 0.3% by weight of the DPI and photosensitizer, respectively. The intensity of the epoxide band at 790 cm^{-1} was monitored, and the percent conversion was calculated point-by-point as a function of irradiation time using standard equations.

Products of the photolysis of the diaryliodonium salts were analyzed by GCMS using a DELSI DI 700 gas chromatograph equipped with a NERMAG R10-10 mass spectrometer.

RESULTS AND DISCUSSION

Photochemistry of DPIs

In Figure 1 are shown the ground state UV absorption spectra of DPIs **1** to **5**. Typically, these compounds exhibit an intense absorption band in the 230–260 nm region (ϵ = ~17,000 $M^{-1} \cdot cm^{-1}$ [8]). It has been shown that placing electron-donating substituents on the aromatic rings of a DPI produces a bathochromic

TABLE 1B. Thioxanthone Photosensitizers

Name	Notation	Structure
2-Chlorothioxanthone	**CTX**	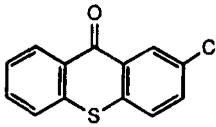
2-Isopropylthioxanthone	**ITX**	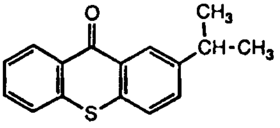
3-Carboethoxy-7-methylthioxanthone	**ETX**	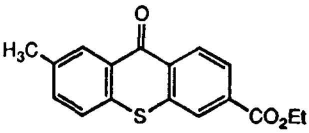
1-Carboethoxy-3-nitrothioxanthone	**T1**	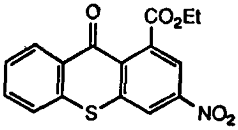
1-Carboxy-3-chlorothioxanthone	**T2**	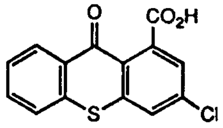
1-Carboethoxy-3-phenylsulfonylthioxanthone	**T3**	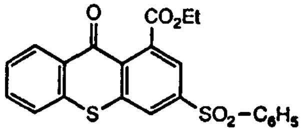
N-Allyl-3,4-imidothioxanthone	**T4**	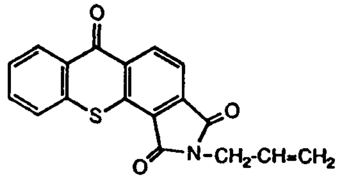

shift, while electron-withdrawing substitutents shift the UV absorption to shorter wavelengths. In all cases the position of the absorption bands indicates that these photoinitiators are primarily photosensitive at the 254 and 313 nm mercury emission bands and not to higher wavelength bands. Characteristic fluorescence spectra for DPIs 1 to 4 are shown in Fig. 2. The quantum yields are very low indicating that radiative deactivation of the singlet excited state by fluorescence is extremely inefficient.

TABLE 1C. Epoxide Monomers Used in These Investigations

Name	Notation	Structure
Bisphenol-A-diglycidyl ether	**MI**	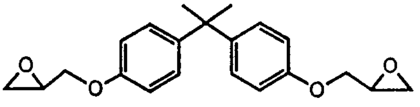
3,4-Epoxycyclohexylmethyl-3′,4′-epoxycyclohexane-carboxylate	**MII**	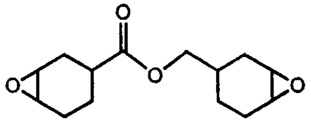

The photolysis of DPIs has been proposed to occur by both a heterolytic and a homolytic cleavage of one of the carbon-iodine bonds which results, respectively, in the formation of an aryl cation–haloarene pair and an aryliodinium cation-radical–aryl radical pair [9, 10]. The mechanism is depicted in Scheme 1.

Excitation by irradiation produces the excited singlet diaryliodonium salt $[Ar_2I^+ X^-]$. This species can undergo a heterolytic cleavage which gives rise to a caged aryl cation–iodoarene pair which is represented in Scheme 1 by a bar over the structure. Intersystem crossing from the excited singlet leads to the excited triplet which can decay to the ground state or undergo homolysis to a caged triplet aryl radical–iodoarene geminate pair. In Scheme 1, the bar denotes that the indicated

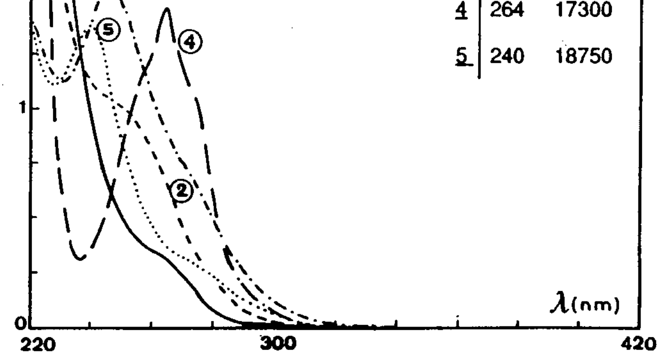

	λ	ε
1	227	17800
2	215	35000
3	218	438
4	264	17300
5	240	18750

FIG. 1. Ground state absorption spectra of **1** to **5** in methanol. Insert: Wavelength of maximum absorption (nm) and molar extinction coefficients ($M^{-1} \cdot cm^{-1}$) [8].

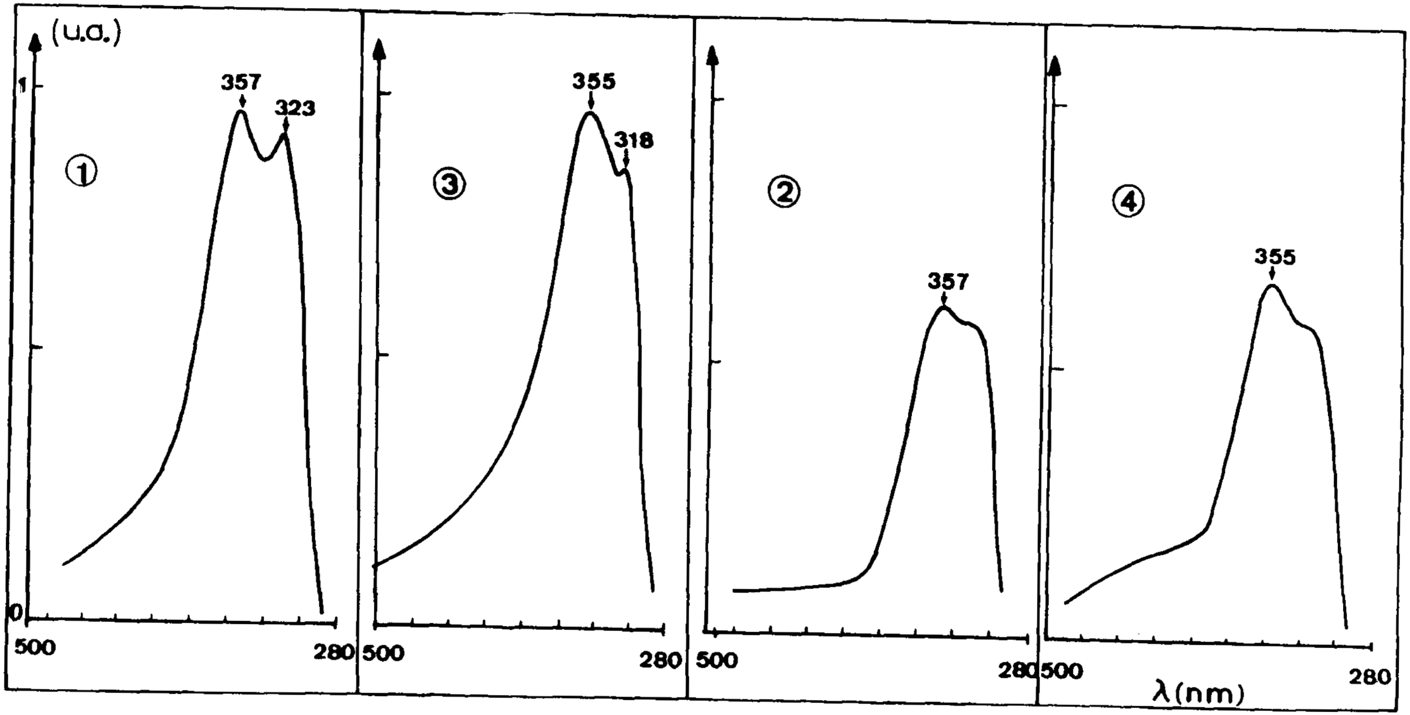

FIG. 2. Fluorescence emission spectra of **2** to **5** in methanol: 1) **2**; 2) **3**; 3) **4**; 4) **5**; λ_{exc} = 255 nm.

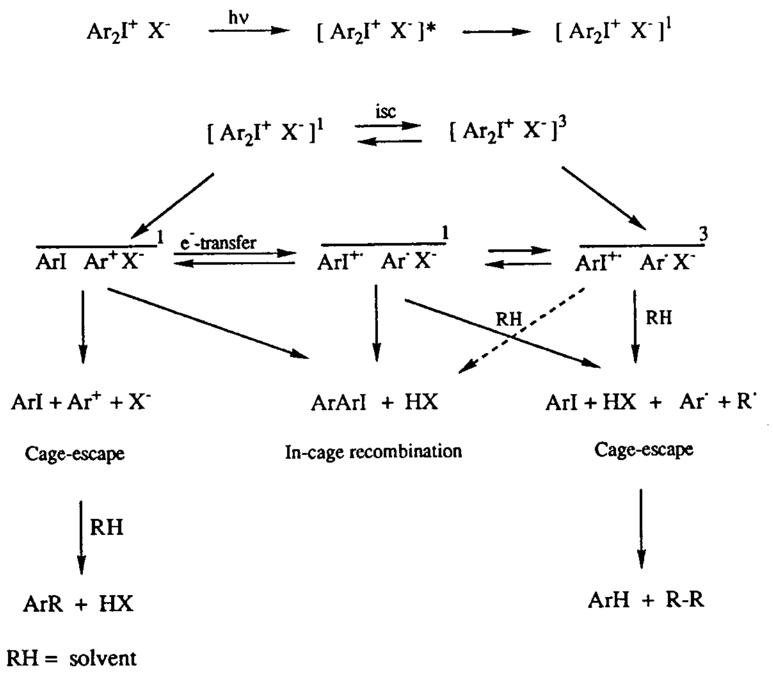

SCHEME 1.

species are generated in a solvent cage. Each of the corresponding caged pairs of reactive intermediates may undergo further reactions depending on whether the reactions occur by an in-cage or cage-escape process. Detailed product analysis has shown that the heterolytic cleavage reaction is the predominant pathway followed in the irradiation of diaryliodonium salts.

In the case of symmetrical diaryliodonium salts, such as **2** and **5**, one cannot discriminate between which of the two carbon-iodine bonds is broken during photolysis. On the other hand, Fig. 3 shows the GCMS of the photolysis products of (4-methoxyphenyl)phenyliodonium hexafluoroarsenate, **3**. The primary products are iodobenzene, anisole, and 4-iodoanisole. In addition, 4-hydroxyanisole and a mixture of isomeric methoxybiphenyls are also formed. Thus, phtotolytic cleavage of both carbon-iodine bonds occurs indiscriminately.

The detection of the reactive intermediates produced during the photolysis of DPIs is rather difficult, and several attempts have been made using flash photolysis [13, 14]. During a study of the flash photolysis of **2**, very weak and long-lived transient absorptions were detected in the UV at approximately λ = 310 nm and in the visible at λ = 600 nm. On the basis of previous flash photolysis studies on diphenyliodonium salts [22], this transient was assigned to the cation radical:

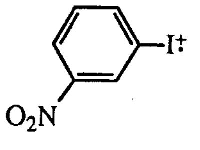

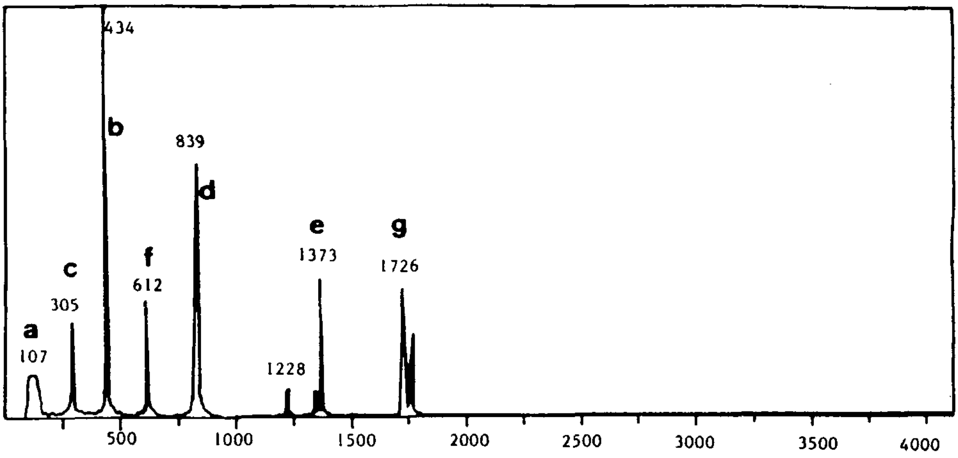

FIG. 3. GCMS chromatogram of an irradiated solution of 3 (10^{-2} M) in methanol: a) solvent; b) iodobenzene; c) anisole; d) iodoanisole; e) methoxybiphenyl; f) *p*-hydroxymethyl anisole; g) 3.

When DPIs are photolyzed, acids are produced which arise via the reactions of the reactive intermediates shown in Scheme 2. These acids are the predominant species responsible for the initiation of cationic photopolymerization by diaryliodonium salts [2]. In addition, cationic polymerization may also occur by the direct attack of aryl cations and aryliodonine cation-radicals on a monomer.

In Table 2 are shown the results of a study of the release of acid by photolysis of DPIs 1–5 in methanol. The measurements of the amount of photogenerated acid were carried out potentiometrically and recorded as the conductivity in millivolts. Some differences in the amount of acid generated can be discerned which can be correlated to the structure of the DPI and its photosensitivity. The cyclic iodonium salt, 4, generates the least amount of acid on photolysis. This is expected since on photolysis the reactive fragments which are formed by photolytic cleavage of one of the carbon-iodine bonds are held in close proximity to one another. This would be expected to facilitate recombination and result in diminished acid production, as shown in Eq. (1).

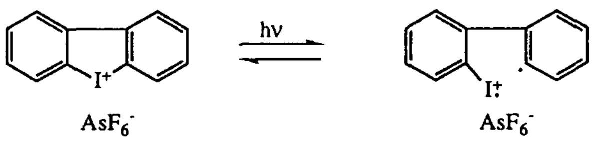

(1)

Other differences seen in Table 2 can be explained on the basis of the UV absorption spectra of the respective DPIs (Fig. 1). Those DPIs having longer wavelength absorption bands together with high molar absorption coefficients such as 3 and 5 generate more acid than photoinitiators such as 2 which have short wavelength absorption bands with low molar absorption coefficients. This is due to the better overlap of the absorption bands of 3 and 5 and the mercury emission bands at 254

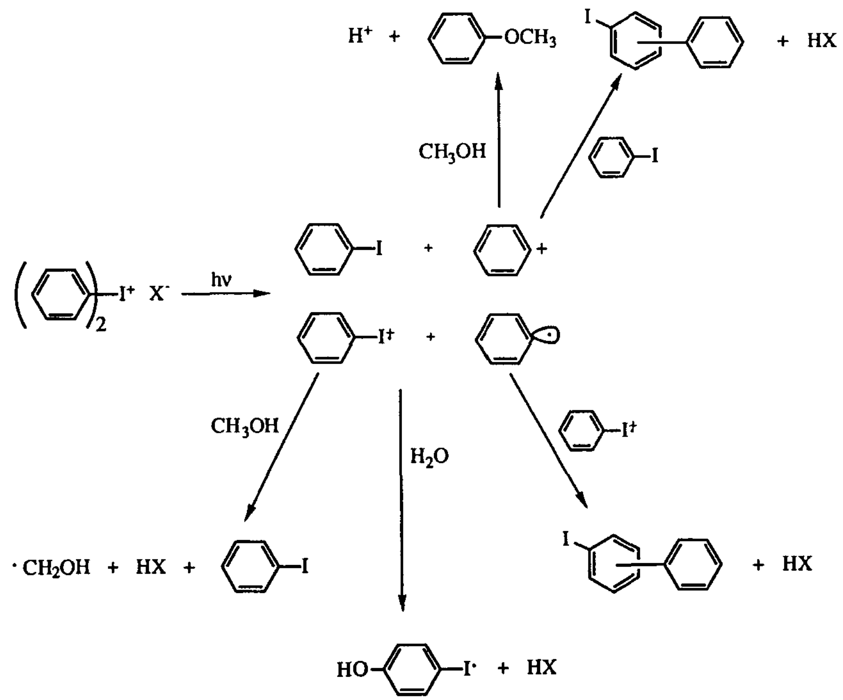

SCHEME 2.

and 313 nm than for DPIs such as **2** which have their major absorption bands at wavelengths below 240 nm.

Photopolymerization Activity of DPIs

The percent conversion of monomer to polymer versus time curves for DPIs **1**–**4** are shown in Figs. 4(A) and 4(B), respectively, for bisphenol-A diglycidyl ether (MI) and the biscycloaliphatic epoxide monomer 3,4-epoxycyclohexylmethyl-3′,4′-epoxycyclohexane carboxylate (MII). The corresponding rates of polymerization, R_p, calculated from the slopes of these curves are listed in Table 3. The results show the strong effects of the substitutents (**2** > **3** > **5**) on the aryl rings and changes in the basic chemical structure (**4**) of the diphenyliodonium salt on the Rp of these two monomers. The results correlate well with the corresponding data from Table 2 which compares the amount of acid released by each of the diaryliodonium salts. It is also clear from Table 3 that the R_p values are in the order **5** > **1** > **3** > **2** > **4** and are independent of the structure of the monomer. In contrast, it was found that the percent conversions for both monomers are a function of the both photoinitiator and the monomer structures with **5** > **3** > **1** > **2** > **4** being the order for MI and **1** > **3** > **5** > **2** > **4** the order for MII. One possible explanation for the low reactivity of cyclic iodonium salt **4** could be due to a poor quantum yield which results in a low efficiency of acid production as noted before in Table 2. Further, it was shown earlier that the reaction of the phenyliododine cation-radical with

TABLE 2. Acidity Release of Solutions of DPIs in Methanol after 1 hour of Irradiation

Product	Structure	E_1 (before irradiation), mV	E_2 (after irradiation), mV	ΔE (mV), $E_2 - E_1$
2	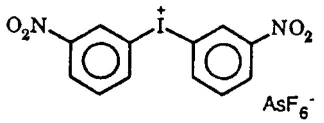	+108	+380	272
3	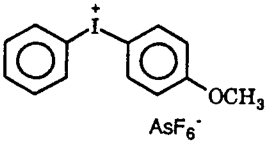	−50	+340	390
4	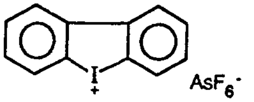	−5	+40	35
5	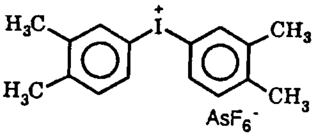	−60	+355	415

cyclohexene oxide and methanol [9] can take two competing pathways. As shown in the following equations, addition of monomer (followed by electron transfer) can take place in competition with reduction. Further, the addition of an aryl cation to the epoxide oxygen can also result in the initiation of polymerization.

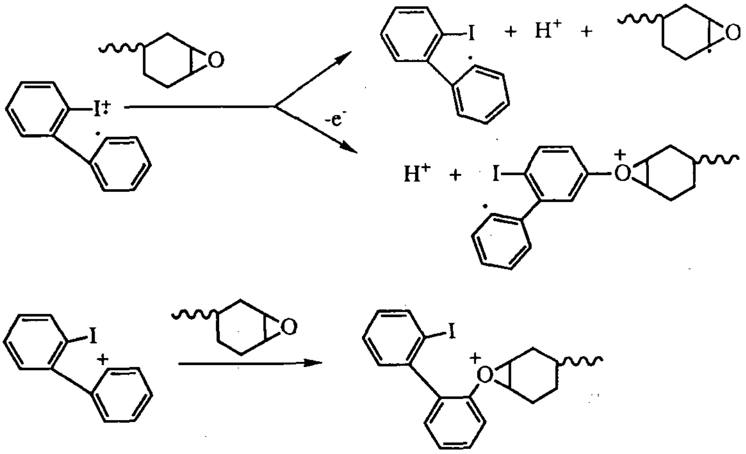

(2,3)

Both of these reactions would be expected to be less efficient for the cyclic iodonium salt photoinitiator **4** on the basis of steric hindrance considerations.

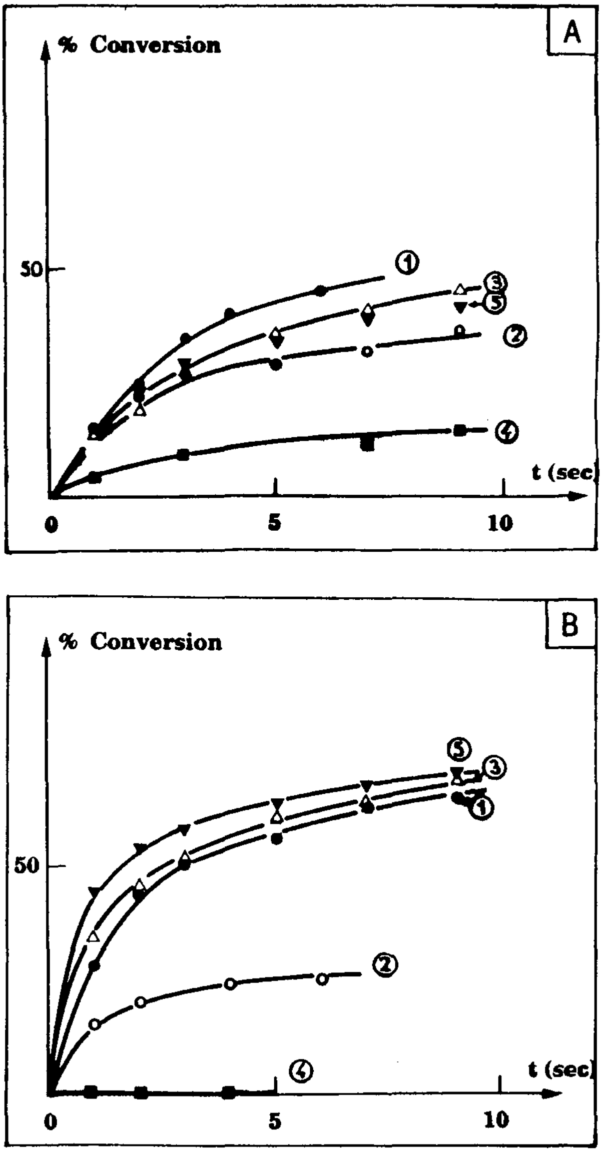

FIG. 4. Photopolymerizations of **MI** (A) and **MII** (B) in the presence of **1** to **5**.

TABLE 3. Rates of Polymerizations of Monomer **MI** and **MII** (in $M \cdot s^{-1}$) in the Presence of **1** to **5**

	1	**2**	**3**	**4**	**5**
R_p(**MI**)	0.82	0.65	0.72	0.21	0.87
R_p(**MII**)	2.91	1.55	4.65	<0.05	5.47

Interactions between DPIs and TX Photosensitizers

Substituted TXs exhibit a strong absorption band in the 250–270 nm region as well as a weaker band at 380–420 nm in the near UV-visible region. These spectral features make TXs very attractive as photosensitizers. Shown in Fig. 5 are the UV absorption curves for a number of TXs of interest in this research.

When a TX is irradiated, a short-lived singlet state, S_1, is formed with a lifetime in the nanosecond range. Very fast intersystem crossing takes place leading to the formation of a long-lived triplet state, T_1, with a lifetime in the range of microseconds. The T_1 states of the excited TXs can be detected by their characteristic broad absorption bands in visible region from approximately 550–700 nm as shown in Fig. 6.

Thioxanthones are known to be active photosensitizers for diaryliodonium salts [8a]. It is most likely that the excited state involved in the photosensitization of these compounds is the T_1 state of the TX. From a kinetic point of view, photosensitization by S_1 states is highly improbable since the rate of intersystem crossing in TX compounds is normally very much faster than the rate of quenching of the S_1 states by singlet quenchers. Moreover, in highly concentrated solutions the relationship shown in Eq. (4) applies due to viscosity effects on $k_q^{S_1}$:

$$k_{\mathrm{ISC}} >> k_Q^{S_1}[\mathrm{DPI}] \qquad (4)$$

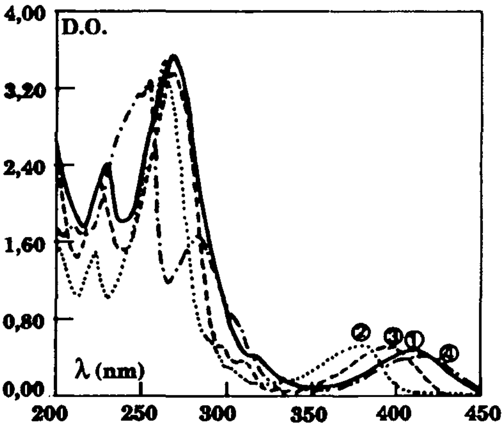

FIG. 5. Characteristic absorption spectra of TXs in acetonitrile: 1) **T1**; 2) **T2**; 3) **T3**; 4) **T4**.

These investigations were carried out in dilute solutions of various solvents, and monomers were used. The situation described by Eq. (4) is even less favorable under these conditions since the overall rate of quenching of S_1 states is dependent on the concentration of the DPI while the rate of intersystem crossing is not. Lastly, in contrast to previous studies [23] which were carried out at high DPI concentrations in polar media, significant fluorescence quenching, which is indicative of the participation of S_1 states in photosensitization, was not observed for a variety of DPI concentrations under the experimental conditions described here.

The rate constants, k_e, for the interaction of the triplet states of a TX with the ground state DPIs can be calculated from the Stern–Volmer quenching plots according to Eq. (5):

$$k = k_0 + k_e[\mathrm{DPI}] \tag{5}$$

where k and k_0 are, respectively, the first-order rate constant of the quenching of the excited triplet of the TX in the presence and absence of DPIs. The Stern–Volmer plots for four substituted and unsubstituted TXs are shown in Fig. 7, and the k_e values calculated from the slopes of these curves are summarized in Table 4. The mechanism of the quenching process, as depicted in Eq. (6), consists of an electron transfer process which takes place by the interaction of the excited TX with the DPI whereby a thioxanthone cation-radical ($TX^{+\cdot}$) and a diaryliodine radical are formed.

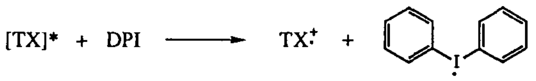

(6)

This mechanism is supported by three independent pieces of evidence. First, the quenching process results in the generation of new absorption bands in the 400–500 nm region, and these have been identified in some cases as being attributable to

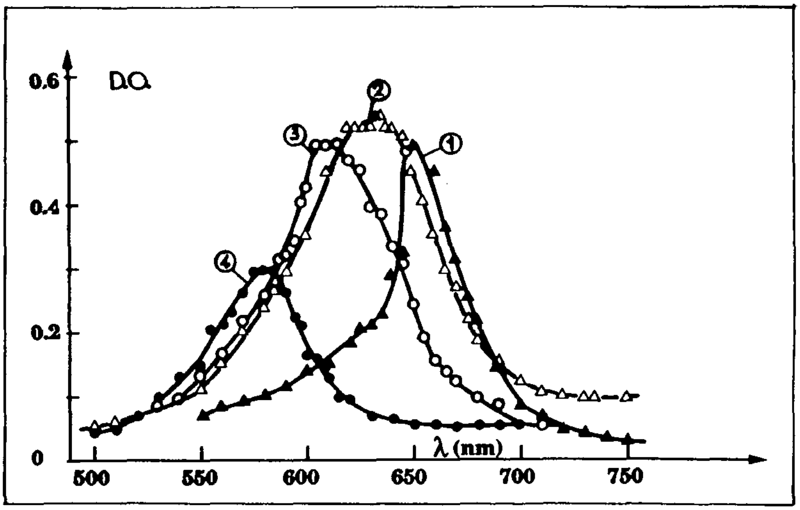

FIG. 6. Transient triplet-triplet absorption spectra of TXs in acetonitrile: 1) **T1**; 2) **T2**; 3) **T3**; 4) **T4**.

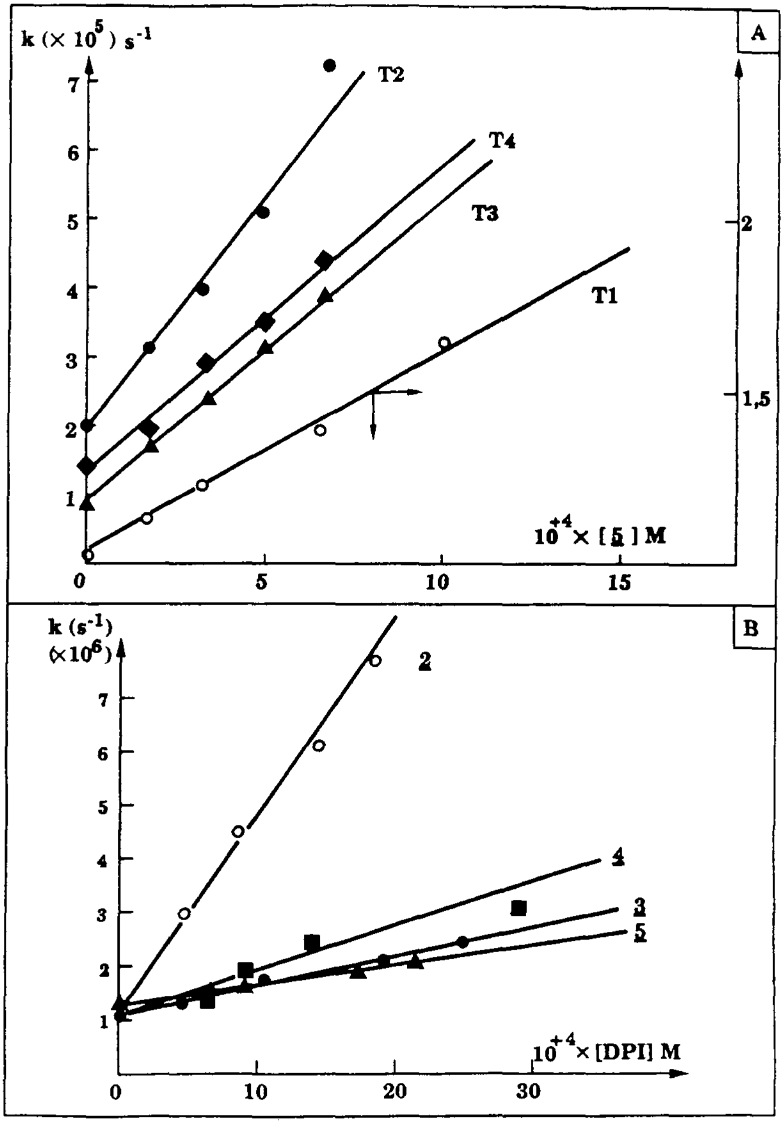

FIG. 7. Typical Stern-Volmer plots for triplet state quenching of different TXs by 5 (A) and CTX by DPIs (B).

thioxanthone cation-radicals [18, 19]. Second, thermodynamic calculations of the free energy using the Rhem-Weller equation as shown in Table 4 give large negative ΔG values, indicative of a facile electron-transfer process for each of the TX photosensitizers studied. Lastly, analysis of the reaction mixtures of the photosensitized photolyses of DPIs by GCMS gives products which can be rationalized as being

TABLE 4. Rate Constants of Quenching of the Triplet States of TX by DPI in Methanol and Acetonitrile. Calculated ΔG Values According to the Rehm–Weller Equation [CTX: $\Delta E^{3}_{0,0}$ = 2.84 eV; $E^{1/2}_{\mathrm{ox}}$ (MeOH): 1.57 V; $E^{1/2}_{\mathrm{ox}}$ (CH_3CN): 1.52 V]

k_e ($M^{-1} \cdot s^{-1}$)	**2**	**3**	**4**	**5**
CTX/MeOH	4×10^9	6.7×10^8	8×10^8	3.6×10^8
ΔG (kJ·mol^{-1})	−103	−105	−109	−104
CTX/CH_3CN	7.8×10^9	2.1×10^9	3.6×10^9	2.5×10^9
ΔG (kJ·mol^{-1})	−108	−109	−114	−109
ITX/MeOH	2.5×10^9	3.3×10^8	8×10^8	2.8×10^8
ETX/MeOH	2.2×10^9	2×10^8	2.5×10^8	2.8×10^8
T1/CH_3CN	5×10^8	4×10^8	1.3×10^8	5.6×10^8
T2/CH_3CN	3.9×10^9	6.2×10^8	7×10^8	6.7×10^8
T3/CH_3CN	1.3×10^9	1.2×10^8	3.3×10^8	4.5×10^8
T3/MeOH			6.3×10^8	
T4/CH_3CN	1.4×10^9	1.2×10^8	3.2×10^8	4.5×10^8

derived from a diaryliodine radical. For example, the irradiation of **3** in methanol in the presence of CTX as a photosensitizer yields iodobenzene, anisole, iodoanisole, and benzene, which can be rationalized as derived from the 4-methoxyphenylphenyliodine radical.

The rate constants for quenching of the triplet state TXs by monomer can be determined by substituting k_q for k_e in the Stern–Volmer equation. Values of 1.0 × 10^7 $m^{-1} \cdot s^{-1}$ were obtained for the systems CTX/**MI** and CTX/**MII**. Thus, the rates of triplet quenching by the epoxy monomers are one to two orders of magnitude less than those observed by interaction of the excited TX with the DPIs.

In contrast to the facile TX triplet quenching by DPIs, no significant quenching of the excited singlet (S_1) state by DPIs was observed for a range of DPI concentrations.

Photosensitized Formation of Acid

Solutions of CTX (OD = 0.4 at 366 nm) containing 10^{-2} M DPIs were exposed to either an unfiltered medium pressure mercury arc lamp or a lamp equipped with a 366-nm bandpass filter. For diaryliodonium salts **3** and **4**, the results shown in Fig. 8 clearly indicate that acid is formed in the photosensitized process since these two DPIs do not absorb at λ = 300 nm. On the other hand, since **2** has appreciable absorption at wavelengths above 360 nm, both direct and photosensitized processes contribute to the production of acid in this case. Due to the low concentrations of DPIs used in this study, the absorption of **2** cannot be seen in Fig. 1. The following sequences of reactions are proposed to explain the photosensitized formation of acids in TX/DPI systems.

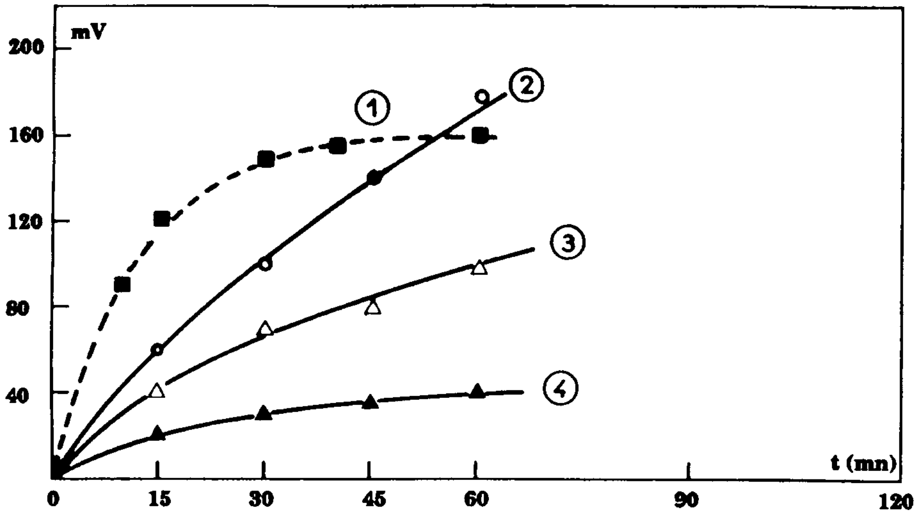

FIG. 8. Acid release in methanolic solution of CTX and DPIs (10^{-2} M) as a function time. 1) **2** (polychromatic light); 2) **2**; 3) **3**; 4) **4**. In experiments 2), 3) and 4), light is filtered at $\lambda = 366$ nm.

$$\begin{array}{l} TX \xrightarrow[DPI]{h\nu} TX^{+\cdot} + DPI^{\cdot} \\ \qquad\quad \xrightarrow{RH} TX + R^{\cdot} + H^{+} \end{array} \tag{7}$$

The thioxanthone cation-radical generated by electron-transfer reaction with the DPI can interact with a proton donor molecule, RH, to give the neutral thioxanthone, a free radical, $R^{\cdot}$, and H^{+} (acid).

Photosensitized Polymerization of Epoxides in Thin Films

The course of the CTX photosensitized cationic polymerizations of **MI** and **MII** in thin films were followed by infrared spectroscopy by monitoring the decrease of the epoxide band at 790 cm^{-1}. Typical infrared curves of the polymerizations at various times are displayed in Fig. 9. Along with a decrease in the epoxide band, there is a concomitant increase in the OH band at 3500 cm^{-1} as shown in Fig. 10. Using these spectra, the conversion versus irradiation time plots depicted in Fig. 11 and rates of polymerization were calculated. Gathered in Table 5 are the rates of polymerization, rate constants of electron transfer and monomer quenching, and the amount of acid produced for the CTX-sensitized polymerizations of **MI** and **MII** with various DPIs. The following general trends were observed:

1. All things considered, the major factor in determining the relative rates of polymerization is the structure of the monomer. **MII** containing two cycloaliphatic epoxy groups is considerably more reactive than the corresponding **MI** possessing two glycidyl ether moieties.

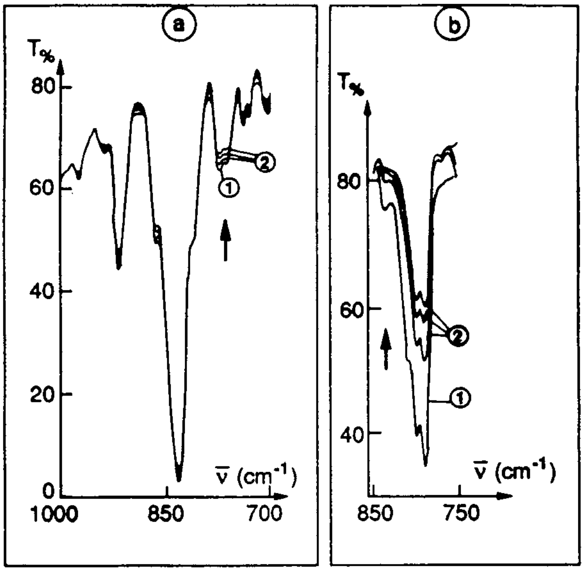

FIG. 9. Evolution of the epoxide IR band of **MI** (a) and **MII** (b) in the presence of CTX/**2** and CTX/**1**, respectively.

2. When polychromatic UV irradiation is used, the contribution of photosensitization to the overall rate of polymerization of monomers **MI** and **MII** is not very significant. The R_p values show only a 1.5 to 2.1-fold increase in the presence of the photosensitizer as compared to when it is absent. Thus, direct photolysis appears to be the major contributor in determining the overall polymerization rates.
3. The most efficient DPI, **2**, with respect to electron-transfer photosensitization rate and amount acid generated, does not lead to the highest R_p. Since, as has been noted before, both **2** and CTX have absorption bands in the same region of the spectrum, this result is most likely due to screening effects in the short wavelength UV by the highly absorbing CTX. The overall effect is to reduce the overall available light necessary for the direct photolysis of **2**.
4. The initiation of cationic polymerization in TX-photosensitized DPI systems result from the direct and indirect interaction of the $TX^{+\cdot}$ cation-radical with the monomer and photoinitiator as depicted in Eqs. (8)–(10).

$$TX^{+\cdot} \xrightarrow{RH} H^+ + R^\cdot + TX \tag{8}$$

$$R^\cdot \xrightarrow{Ph_2I^+X^-} R^+X^- + Ph_2I^\cdot \tag{9}$$

$$H^+ \text{ or } R^+ \xrightarrow{M} H(M)_nM^+ \tag{10}$$

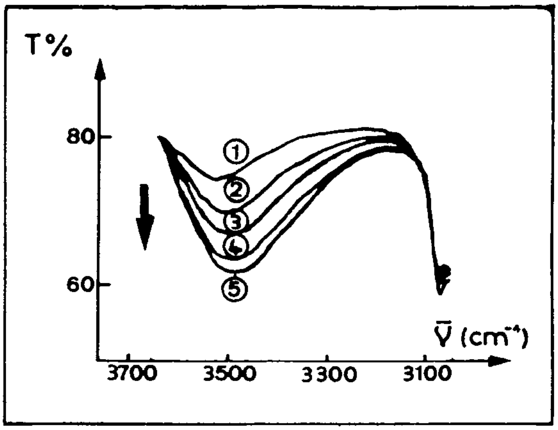

FIG. 10. Evolution of the OH IR band as a function of the irradiation time: 1) $t = 0$; 2) $t = 1$ second; 3) $t = 2$ seconds; 4) $t = 3$ seconds; 5) $t = 4$ seconds; monomer 1, iodonium salt: 1.

In this scheme, RH is a proton donor, usually the monomer. The first reaction (Eq. 8) consists of the interaction of a thioxanthone cation-radical with the monomer or solvent to generate a neutral thioxanthone molecule, a solvent or monomer-derived free radical and a proton. In the second step (Eq. 9), the free radical can reduce the iodonium salt. The overall results of this reaction are the formation of a cation and fragments from decomposition of the diaryliodonium free radical. Subsequently, the R^+ cation can react with solvent to give protons which can initiate polymerization by direct attack on the epoxy monomer resulting in ring-opening polymerization as depicted in Eq. (10). Further reactions may also take place between the various reactive fragments generated in Eqs. (8)-(10) which contribute to acid generation. These are shown in Eqs. (11) and (12).

$$TX^{+\cdot} + R^{\cdot} \longrightarrow R{-}TX\,(+H^+) \tag{11}$$

$$TX^{+\cdot} + Ph_2I^{\cdot} \longrightarrow Ph{-}TX + Ph\text{-}I + H^+ \tag{12}$$

In contrast to the above photosensitized polymerization which depends ultimately on the reactivity of the thioxanthone cation-radical, the species responsible for the initiation of polymerization in the direct photolysis of diaryliodonium salts are aryl cations and aryliodine cation-radicals. These highly reactive species very rapidly react directly and indirectly with the monomer to initiate cationic polymerization. In contrast, thioxanthone cation-radicals are resonance stabilized, relatively long-lived species. Thus, they are less reactive toward attack on the monomer as well as in reactions which generate protons. This rationale may account for the difference in efficiency between the direct and photosensitized cationic polymerizations.

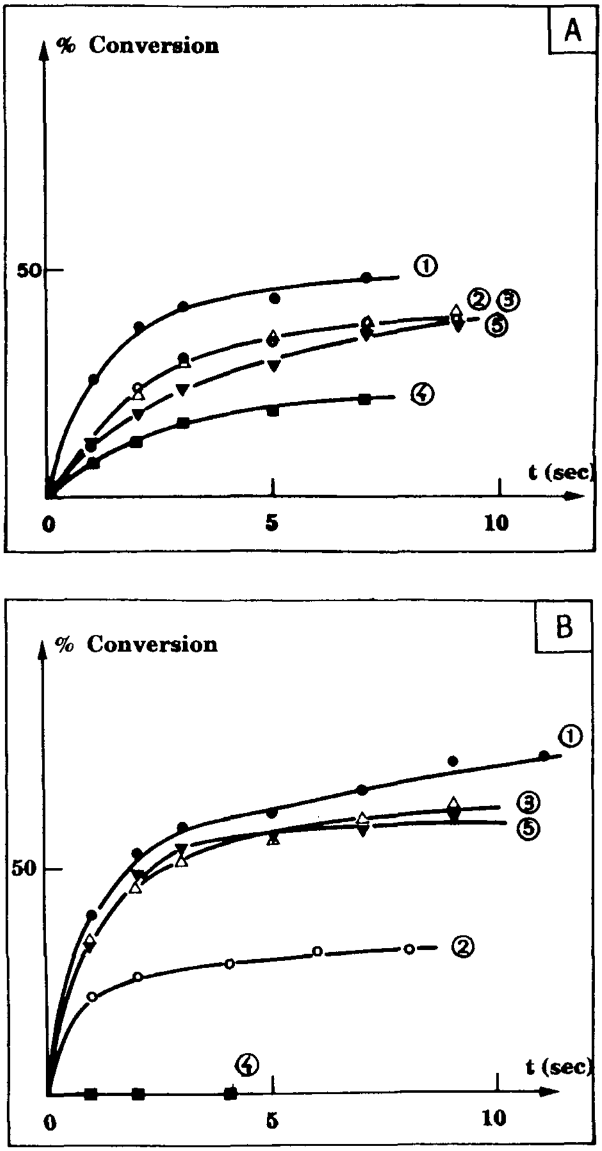

FIG. 11. Photosensitized polymerizations of **MI** (A) and **MII** (B) in the presence of CTX/DPIs: 1) **1**; 2) **2**; 3) **3**; 4) **4**; 5) **5**.

TABLE 5. Sensitized Photopolymerization Reactions of **MI** and **MII** in the Presence of CTX/DPIs. Rate Constants of Quenching of the CTX Triplet State by DPIs (k_e) and Monomer k_q, Rates of Polymerization R_p ($M \cdot s^{-1}$), Acid Release Δ, Yield of Electron Transfer in the Presence of **MI** and **MII**. [**MI**] = 3 M; [**MII**] = 4.7 M; [epoxide] = 2 [**MI**] or 2 [**MII**]

CTX	k_e	k_q	R_p(MII)	R_p(MI)	Δ, mV	ϕ_e(MII)	ϕ_e(MI)
1	2.4×10^8	–	4.89	1.72	–	0.24	0.15
2	4.0×10^9	–	2.33	0.72	(180)	0.81	0.70
3	6.7×10^8	–	4.65	0.72	100	0.45	0.31
4	8.0×10^8	–	<0.05	0.41	40	0.52	0.37
5	3.6×10^8	–	5.47	0.87	–	0.31	0.18
MI	–	1×10^7	–	–	–	–	–
MII	–	0.4×10^7	–	–	–	–	–

5. Photoinitiated cationic polymerization can be initiated in the near UV-visible region of the spectrum using **T1** or **T4** as photosensitizers. These compounds should be efficient photosensitizers at λ = 441 nm which is the wavelength delivered by either a He/Cd laser or by a laser-pumped dye laser [21]. Thus, TX photosensitized cationic polymerizations could be used for such applications as direct laser imaging and writing processes which employ these emission sources.

Reactivity of a Longer Wavelength Absorbing Iodonium Salt

The substitution of one of the phenyl rings in diphenyliodonium salts with the fluorenone moiety as shown in photoinitiator **6** leads to the generation of two long wavelength absorption bands at λ_{max} = 294 and 378 nm (ϵ = 8280 and 700 $M^{-1} \cdot cm^{-1}$) in the midregion of the UV. Both the absorption and the fluorescence spectra of **6** closely resemble those of fluorenone as shown in Figs. 12A and 12B, respectively. The photolysis of **6** was carried out in methanol, and the products were characterized by GCMS analysis. Based on the results of this study, a mechanism depicted in Scheme 3 involving the intramolecular photosensitization of **6** has been proposed.

A long-lived triplet state is generated on photoexcitation of **6**. This may be seen in the triplet-triplet absorption spectrum displayed in Fig. 13. The decay of the triplet state exhibited first-order rate behavior with a rate constant of 3.3×10^5 s^{-1} in methanol.

The photopolymerization of films of **MI** and **MII** were carried out using DPI **6**, and the course of the polymerizations was followed by infrared spectroscopy. In Fig. 14 the percent conversions of monomer to polymer are plotted against time for the two monomers. A comparison of the curves shown in Fig. 14 with those in Fig. 4 shows that despite the longer wavelength absorption of **6**, the rates of polymerization of either **MI** or **MII** using this photoinitiator are not better than those of the other photoinitiators, such as **3** or **5**. The reason for these results may be related to a low cleavage efficiency for **6**.

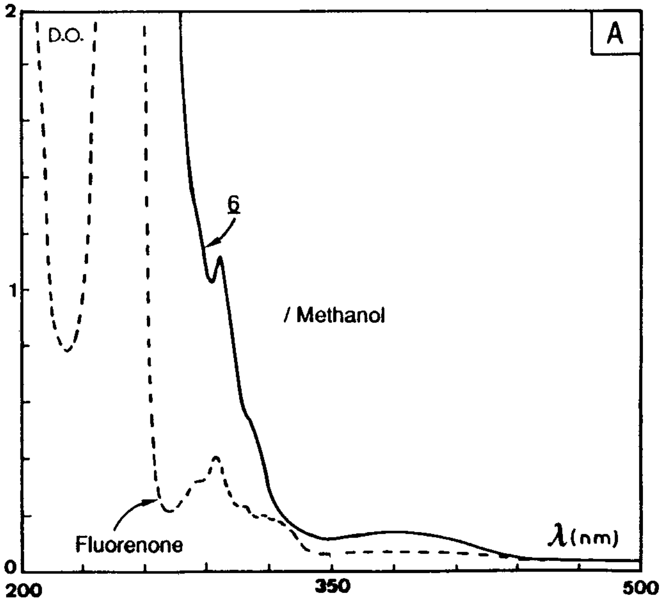

FIG. 12A. Absorption spectra of **6**.

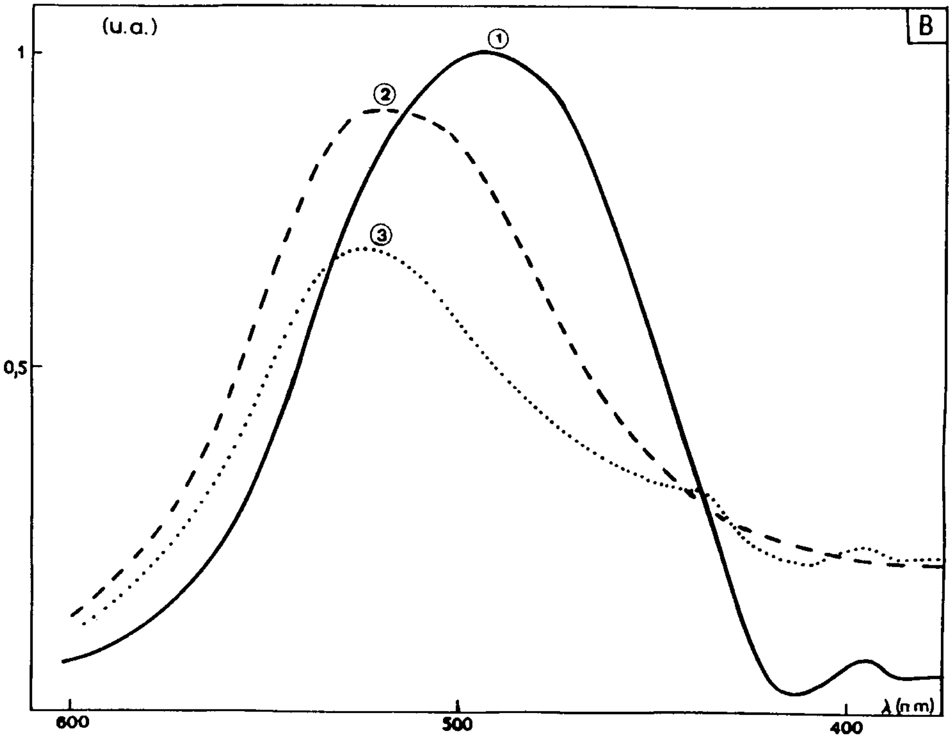

FIG. 12B. Emission spectra of **6** in acetonitrile (1), isopropanol (2), and methanol (3).

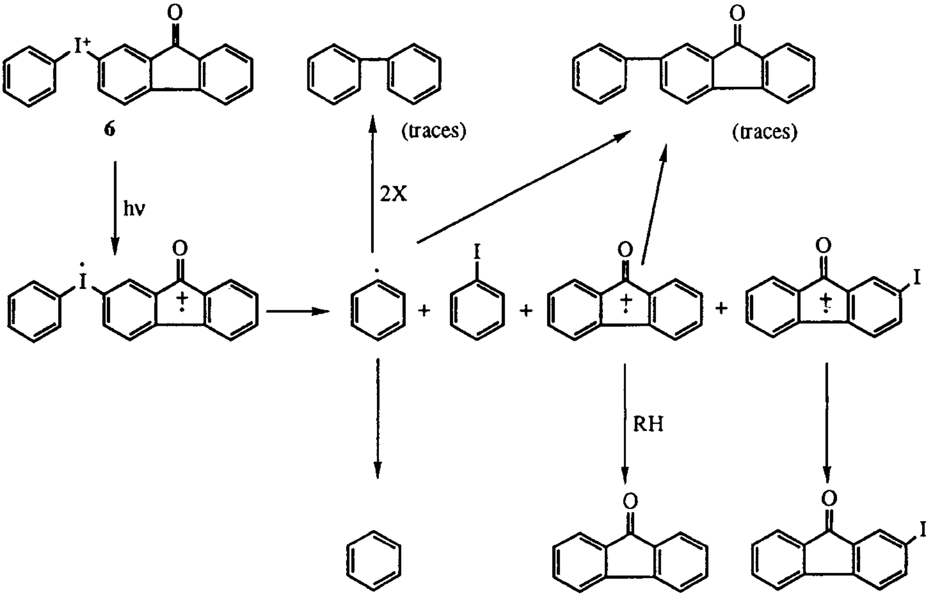

SCHEME 3.

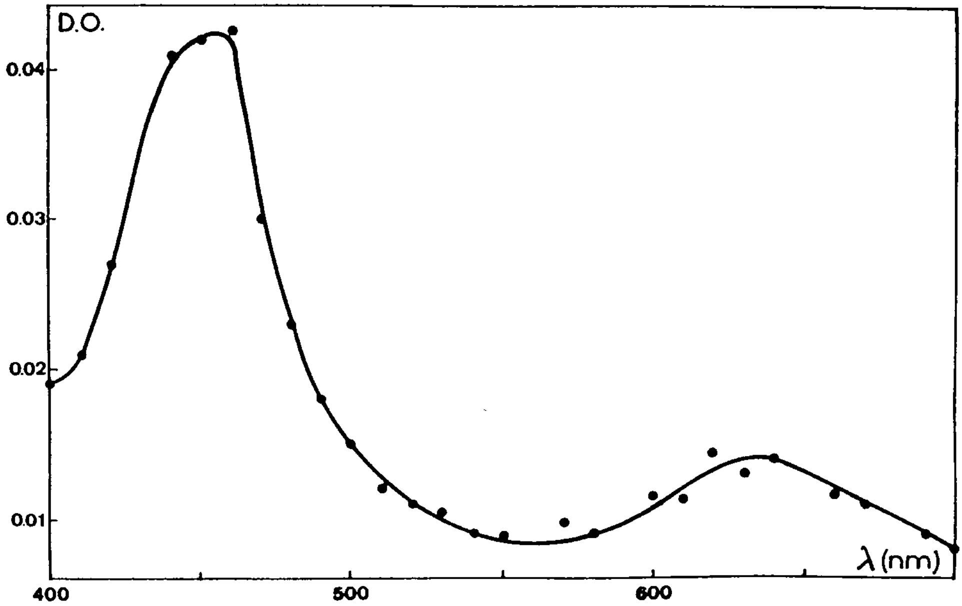

FIG. 13. Triplet-triplet absorption spectrum of **6** in CH_3CN.

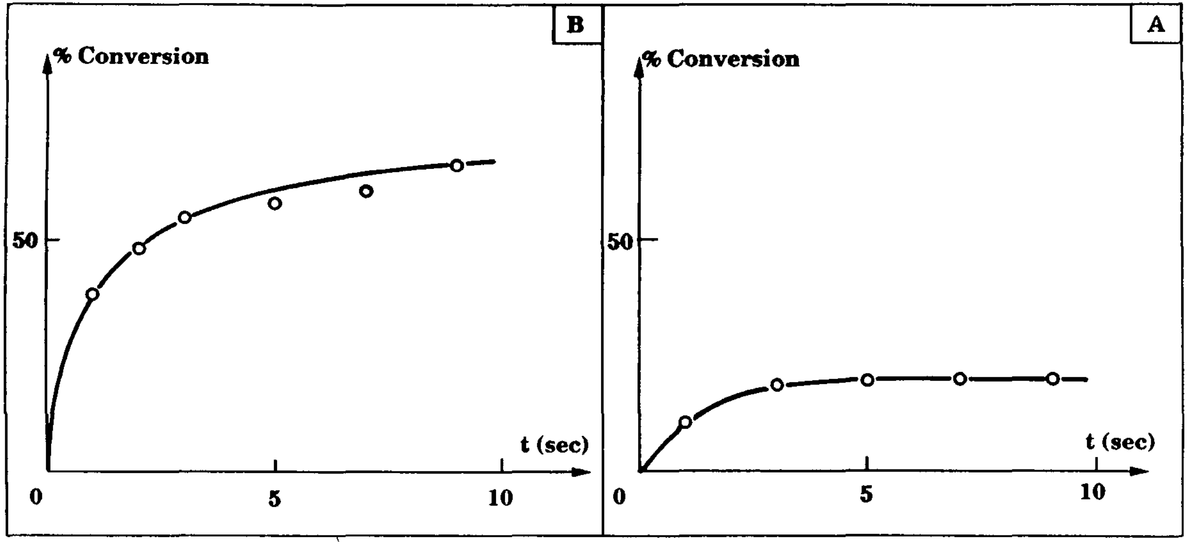

FIG. 14. Percent conversion vs time curves for the photopolymerization of **MI** (A) and **MII** (B) in the presence of **6**. Rates of polymerization are 0.58 $M \cdot s^{-1}$ (A) and 3.88 $M \cdot s^{-1}$ (B).

CONCLUSIONS

Although strong interactions in the excited states are observed when using combinations of DPIs and TXs, the rates of the cationic photopolymerizations of difunctional epoxy monomers is little enhanced compared to the same polymerizations carried out in the absence of a photosensitizer. Investigation of the processes involved in other photoinitiator-photosensitizer combinations is now under way.

REFERENCES

[1] J. F. Rabek, *Mechanisms of Photophysical and Photochemical Reactions in Polymers: Theory and Practical Applications*, Wiley, New York, 1987.

[2] J. V. Crivello, *UV-Curing: Science and Technology* (S. P. Pappas, Ed.), Technology Marketing Corporation, Stamford, Connecticut, 1978.

[3] C. G. Roffey, *Photopolymerization of Surface Coatings*, Wiley, New York, 1982.

[4] J. P. Fouassier, *Photopolymerization and Photoimaging Science and Technology* (N. S. Allen, Ed.), Elsevier Applied Science, 1989, p. 209.

[5] W. Schnabel, *J. Radiat. Curing*, *13*, 1 (1986).

[6] J. P. Fouassier, *Focus on Photophysics and Photochemistry* (J. F. Rabek, Ed.), CRC Press, 1989.

[7] J. P. Fouassier, *Proc. Radiation Technologies, Florence*, Radtech Europe Ed., Fribourg, 1989, p. 33.

[8] (a) J. V. Crivello, *Adv. Polym. Sci.*, *62*, 1 (1984); (b) J. V. Crivello and J. H. W. Lam, *Macromolecules*, *10*(6), 1307 (1977); (c) J. V. Crivello and J. L. Lee, *J. Polym. Sci.*, *Polym. Chem. Ed.*, *28*, 479 (1990).

[9] S. P. Pappas, *Prog. Org. Coat.*, *13*, 35 (1985).

[10] J. L. Dektar and N. P. Hacker, *J. Am. Chem. Soc.*, *112*, 6004 (1990).

[11] D. T. Breslin and F. D. Saeva, *J. Org. Chem.*, *53*, 713 (1988).

[12] J. L. Dektar and N. P. Hacker, *Ibid.*, *56*, 1838 (1991).

[13] R. J. Devoe, M. R. V. Sahyun, N. Serpone and D. K. Sharma, *Can. J. Chem.*, *65*, 2342 (1987).

[14] Y. Yagci, S. P. Pappas, and W. Schnabel, *Z. Naturforsch.*, *42a*, 1425 (1987).

[15] J. L. Dektar and N. P. Hacker, *J. Org. Chem.*, *55*, 639 (1990).

[16] H. J. Timpe and A. G. Rajendran, *Makromol. Chem., Rapid Commun.*, *9*, 399 (1988).

[17] Y. Yagci and W. Schnabel, *Ibid.*, *8*, 209 (1987).

[18] J. P. Fouassier, D. Burr, and J. V. Crivello, *J. Photochem.*, *49*, 318 (1989).

[19] G. Manivannan and J. P. Fouassier, *J. Polym. Sci.*, *Part A*, *29*, 1113 (1991).

[20] J. P. Fouassier, G. Manivannan, and J. V. Crivello, *J. Polym. Sci.*, *Polym. Chem. Ed.*, *30*, 1999 (1992).

[21] D. J. Lougnot, J. P. Fouassier, and J. Faure, *J. Chem. Phys.*, *72*, 125 (1975); J. P. Fouassier, D. J. Lougnot, A. Payerne, and F. Wieder, *Chem. Phys. Lett.*, *135*(1,2), 30 (1987).

[22] M. Tilley, B. Pappas, S. P. Pappas, Y. Yagci, W. Schnabel, and J. K. Thomas, *Imaging Sci.*, *33*(2), 62 (1989).
[23] H.-J. Timpe, K.-P. Kronfeld, U. Lammel, J.-P. Fouassier, and D.-J. Lougnot, *J. Photochem. Photobiol.*, *51*, 111 (1990).

Received July 26, 1993
Revision received August 31, 1993